THE JOURNAL OF BIOLOGICAL CHEMISTRY VOL. 281, NO. 38, pp. 28254–28264, September 22, 2006

Interaction of STIM1 with Endogenously Expressed Human Canonical TRP1 upon Depletion of Intracellular Ca^{2+} Stores*

Received for publication, May 4, 2006, and in revised form, July 26, 2006 Published, JBC Papers in Press, July 26, 2006, DOI 10.1074/jbc.M604272200

José J. López[1], **Ginés M. Salido, José A. Pariente, and Juan A. Rosado**[2]

From the Department of Physiology (Cellular Physiology Research Group), University of Extremadura, 10071 Cáceres, Spain

STIM1 (stromal interaction molecule 1) has recently been proposed to communicate the intracellular Ca^{2+} stores with the plasma membrane to mediate store-operated Ca^{2+} entry. Here we describe for the first time that Ca^{2+} store depletion stimulates rapid STIM1 surface expression and association with endogenously expressed human canonical TRP1 (hTRPC1) independently of rises in cytosolic free Ca^{2+} concentration. These events require the support of the actin cytoskeleton in human platelets, as reported for the coupling between type II inositol 1,4,5-trisphosphate receptor in the Ca^{2+} stores and hTRPC1 in the plasma membrane, which has been suggested to underlie the activation of store-operated Ca^{2+} entry in these cells. Electrotransjection of cells with anti-STIM1 antibody, directed toward the N-terminal sequence that includes the Ca^{2+}-binding region, prevented the migration of STIM1 toward the plasma membrane, the interaction between STIM1 and hTRPC1, the coupling between hTRPC1 and type II inositol 1,4,5-trisphosphate receptor, and reduced store-operated Ca^{2+} entry. These findings provide evidence for a role of STIM1 in the activation of store-operated Ca^{2+} entry probably acting as a Ca^{2+} sensor.

Cellular stimulation by a number of agonists results in an increase in the intracellular free Ca^{2+} concentration ($[Ca^{2+}]_i$), which consists of two components: Ca^{2+} release from finite intracellular stores and Ca^{2+} entry through plasma membrane (PM)[3] channels, which is often required for full activation of cellular functions (1–3). Store-operated Ca^{2+} entry (SOCE), a major mechanism for Ca^{2+} entry in nonexcitable cells, is a process controlled by the filling state of the intracellular Ca^{2+} stores (4); however, the mechanism by which the filling state of the intracellular stores is communicated to the PM remains partially understood.

Several hypotheses have been presented to explain the activation of SOCE, which involves the release of a putative calcium influx factor from the endoplasmic reticulum (ER; indirect coupling), the insertion of Ca^{2+}-permeable channels into the PM, and a direct or conformational coupling. The last suggests a physical interaction between a Ca^{2+} channel in the PM and a protein in the ER, which might be constitutive (the classic conformational coupling model) or reversible and regulated by the actin cytoskeleton upon store depletion (the *de novo* conformational coupling model (3, 5–7)).

Transient receptor potential channels (TRPCs) have been presented as candidates for the conduction of SOCE (8–10), and a functional coupling between TRPCs and various inositol 1,4,5-trisphosphate receptor isoforms (IP_3Rs) has been demonstrated in transfected cells and cells naturally expressing TRPCs (9, 11–13). These studies are in agreement with recent works reporting a role for the protein junctate in the activation of SOCE. This protein has been shown to induce and stabilize coupling between IP_3Rs and bovine TRPC3 (14) and murine TRPC2 and TRPC5 (15).

The ER is a spatially and functionally heterogeneous organelle with nonuniform distribution of endoplasmic Ca^{2+}-handling proteins, including Ca^{2+}-binding proteins, pumps, and channels. Extracellular stimuli may induce the generation of dynamic ER compartments containing Ca^{2+}-handling proteins that may function as "induced coupling domains" between the ER and PM, thereby facilitating Ca^{2+} entry into the cell (16). Among the Ca^{2+}-handling proteins present in the ER, the stromal interaction molecule 1 (STIM1; formerly designated GOK) protein has recently been presented as a messenger linking the ER to PM Ca^{2+} channels. STIM1 is a Ca^{2+}-binding protein located both in the PM and intracellular membranes, including the ER (17, 18) with a single transmembrane region and an EF-hand domain in the N terminus located in the lumen of the ER (18), that might, therefore, function as a Ca^{2+} sensor in the ER (19, 20). Consistent with this, Ca^{2+} channels in the PM are activated when STIM1 is unable to bind Ca^{2+} (21). Knockdown of STIM1 by RNAi reduces SOCE in HEK293, HeLa, and Jurkat T cells (18, 19) and I_{crac} in Jurkat T cells (19). In addition, expression of EF-hand mutants of STIM1 activates SOCE in *Drosophila* S2 and Jurkat T cells (21). STIM1 has been shown to translocate to the PM upon Ca^{2+} store depletion (21).

In the present study, we have investigated the interaction of STIM1 with endogenously expressed hTRPC1 at resting

* This work was supported by Ministerio de Educación y Ciencia-Dirección General de Investigación (MEC-DGI) Grant BFU2004-00165. The costs of publication of this article were defrayed in part by the payment of page charges. This article must therefore be hereby marked "*advertisement*" in accordance with 18 U.S.C. Section 1734 solely to indicate this fact.

[1] Supported by Dirección General de Investigación (DGI) Fellowship BES-2005-6899.

[2] To whom correspondence should be addressed: Dept. of Physiology, University of Extremadura, Cáceres 10071, Spain. Tel.: 34-927257154; Fax: 34-927257110; E-mail: jarosado@unex.es.

[3] The abbreviations used are: PM, plasma membrane; Cyt D, cytochalasin D; ER, endoplasmic reticulum; HBS, HEPES-buffered saline; hTRPC1, human canonical TRP1; TRPC, transient receptor potential channel; Iono, ionomycin; IP_3R, inositol 1,4,5-trisphosphate receptor; PBS, phosphate-buffered saline; SB, Söerscen's buffer; SOCE, store-operated calcium entry; AM, acetoxymethyl ester; TG, thapsigargin; BAPTA, 1,2-bis(2-aminophenoxy)ethane-*N*,*N*,*N*′,*N*′-tetraacetic acid; FITC, fluorescein isothiocyanate.

conditions and upon store depletion and the effect of $[Ca^{2+}]_i$ in this process. In addition, we have investigated the role of STIM1 in the activation of SOCE. Our results indicate that Ca^{2+} store depletion stimulates rapid STIM1 surface expression and association with hTRPC1 independently of rises in $[Ca^{2+}]_i$. These events require the support of the actin cytoskeleton. Electrotransjection with anti-STIM1 antibody prevented the interaction of STIM1 with hTRPC1 and, as well as incubation of nonelectropermeabilized cells with anti-STIM1 antibody, reduced SOCE. These findings are compatible with membrane trafficking underlying *de novo* coupling of IP_3RII to hTRPC1.

EXPERIMENTAL PROCEDURES

Materials—Fura-2 acetoxymethyl ester (fura-2/AM) and calcein/AM were from Molecular Probes (Leiden, The Netherlands). Apyrase (grade VII), aspirin, thrombin, thapsigargin (TG), leupeptin, benzamidine, phenylmethylsulfonyl fluoride, dimethyl-BAPTA, SDS, and bovine serum albumin were from Sigma. Ionomycin (Iono) and cytochalasin D (Cyt D) were from Calbiochem. Anti-STIM1 antibody was from BD Biosciences. Anti-hTRPC1 polyclonal antibody was obtained from Alomone Laboratories (Jerusalem, Israel). Anti-IP_3R type II polyclonal antibody (C-20), horseradish peroxidase-conjugated goat anti-rabbit IgG antibody, horseradish peroxidase-conjugated donkey anti-goat IgG antibody, and fluorescein isothiocyanate (FITC)-conjugated donkey anti-rabbit IgG antibody were from Santa Cruz Biotechnology, Inc. (Santa Cruz, CA). Horseradish peroxidase-conjugated ovine anti-mouse IgG antibody (NA931) was from Amersham Biosciences. Protein A-agarose was from Upstate Biotechnology, Inc. (Madrid, Spain). Enhanced chemiluminescence detection reagents, immobilized streptavidin gel, and EZ-Link™ Sulfo-NHS-LC-Biotin were from Pierce. Hyperfilm ECL was from Amersham Biosciences. All other reagents were of analytical grade.

Platelet Preparation—Platelet suspensions were prepared as previously described (22) as approved by local ethical committees and in accordance with the Declaration of Helsinki. Briefly, blood was obtained from healthy drug-free volunteers and mixed with one-sixth volume of acid/citrate dextrose anticoagulant containing 85 mM sodium citrate, 78 mM citric acid, and 111 mM D-glucose. Platelet-rich plasma was then prepared by centrifugation for 5 min at 700 × *g*, and aspirin (100 μM) and apyrase (40 μg/ml) were added. For loading with dimethyl-BAPTA, cells were incubated for 30 min at 37 °C with 10 μM dimethyl-BAPTA-AM. Cells were then collected by centrifugation at 350 × *g* for 20 min and resuspended in HEPES-buffered saline (HBS), pH 7.45, containing 145 mM NaCl, 10 mM HEPES, 10 mM D-glucose, 5 mM KCl, 1 mM $MgSO_4$ and supplemented with 0.1% bovine serum albumin and 40 μg/ml apyrase.

Cell viability was assessed using calcein and trypan blue. For calcein loading, cells were incubated for 30 min with 5 μM calcein-AM at 37 °C and centrifuged, and the pellet was resuspended in fresh HBS. Fluorescence was recorded from 2-ml aliquots using a Cary Eclipse Spectrophotometer (Varian Ltd., Madrid, Spain). Samples were excited at 494 nm, and the resulting fluorescence was measured at 535 nm. The results obtained with calcein were confirmed using the trypan blue exclusion technique. 95% of cells were viable in our platelet preparations.

Measurement of $[Ca^{2+}]_i$—Human platelets were loaded with fura-2 by incubation with 2 μM fura-2/AM for 45 min at 37 °C. Fluorescence was recorded from 2-ml aliquots of magnetically stirred cellular suspension (2×10^8 cells/ml) at 37 °C using a Cary Eclipse Spectrophotometer (Varian Ltd., Madrid, Spain) with excitation wavelengths of 340 and 380 nm and emission at 505 nm. Changes in $[Ca^{2+}]_i$ were monitored using the fura-2 340/380 fluorescence ratio and calibrated according to a established method (23).

Ca^{2+} entry was estimated using the integral of the rise in $[Ca^{2+}]_i$ for 2.5 min after the addition of $CaCl_2$ (22). Ca^{2+} entry was corrected by subtraction of the $[Ca^{2+}]_i$ elevation due to leakage of the indicator. Ca^{2+} release by TG + Iono was estimated using the integral of the rise in $[Ca^{2+}]_i$ for 3 min after the addition of the agents (22). Ca^{2+} entry and release are expressed as nM·s, as previously described (24, 25).

Immunoprecipitation and Western Blotting—The immunoprecipitation and Western blotting were performed as described previously (22). Briefly, 500-μl aliquots of platelet suspension (2×10^9 cell/ml) were lysed with an equal volume of radioimmune precipitation buffer, pH 7.2, containing 316 mM NaCl, 20 mM Tris, 2 mM EGTA, 0.2% SDS, 2% sodium deoxycholate, 2% Triton X-100, 2 mM Na_3VO_4, 2 mM phenylmethylsulfonyl fluoride, 100 μg/ml leupeptin, and 10 mM benzamidine. Aliquots of platelet lysates (1 ml) were immunoprecipitated by incubation with 2 μg of anti-hTRPC1, anti-STIM1, or anti-IP_3R type II antibody and 25 μl of protein A-agarose overnight at 4 °C on a rocking platform. The immunoprecipitates were resolved by 8% SDS-PAGE, and separated proteins were electrophoretically transferred onto nitrocellulose membranes for subsequent probing. Blots were incubated overnight with 10% (w/v) bovine serum albumin in Tris-buffered saline with 0.1% Tween 20 to block residual protein binding sites. Immunodetection of STIM1, hTRPC1, and IP_3R type II was achieved using the anti-STIM1 antibody diluted 1:250 in TBST for 2 h, the anti-hTRPC1 antibody diluted 1:200 in TBST for 1 h, or the anti-IP_3R type II antibody diluted 1:500 in TBST for 3 h. The primary antibody was removed, and blots were washed six times for 5 min each with TBST. To detect the primary antibody, blots were incubated for 45 min with horseradish peroxidase-conjugated ovine anti-mouse IgG antibody, horseradish peroxidase-conjugated donkey anti-rabbit IgG antibody, or horseradish peroxidase-conjugated donkey anti-goat IgG antibody diluted 1:10,000 in TBST and then exposed to enhanced chemiluminescence reagents for 4 min. Blots were then exposed to photographic films. The density of bands on the film was measured using a scanning densitometry.

Subcellular Fractionation—Human platelet fractionation was carried out as described previously (26). Briefly, activated and control platelets (2×10^9 cells/ml) were immediately lysed with an equal volume of 2× Triton buffer (2% Triton X-100, 2 mM EGTA, 100 mM Tris/HCl (pH 7.2), 100 μg/ml leupeptin, 2 mM phenylmethylsulfonyl fluoride, 10 mM benzamidine, 2 mM Na_3VO_4) at 4 °C for 30 min. Platelet lysate was centrifuged at 16,000 × *g* for 5 min. The supernatant (cytosolic and membrane fraction) was removed, and the pellet (cytoskeleton-rich

fraction) was solubilized into the original volume in Laemmli's buffer (22), boiled for 5 min, and subjected to Western blotting as described previously.

Immunofluorescence—Samples of platelet suspension (200 μl; 2×10^8 cells/ml) were transferred to 200 μl of ice-cold 3% (w/v) formaldehyde in PBS for 10 min and then incubated for 2 h with 1 μg/ml anti-STIM1 antibody. The platelets were then collected by centrifugation and washed twice in phosphate-buffered saline (PBS) containing 137 mM NaCl, 2.7 mM KCl, 5.62 mM Na_2HPO_4, 1.09 mM NaH_2PO_4, 1.47 mM KH_2PO_4, pH 7.2, and supplemented with 0.5% (w/v) bovine serum albumin. To detect the primary antibody, samples were incubated with 0.02 μg/ml FITC-conjugated donkey anti-rabbit IgG antibody for 1 h and washed twice in PBS. Fluorescence was measured using a fluorescence spectrophotometer (PerkinElmer Life Sciences). Samples were excited at 496 nm, and emission was at 516 nm.

Reversible Electroporation Procedure—The platelet suspension was transferred to an electroporation chamber containing antibodies at a final concentration of 2 μg/ml, and the antibodies were transjected according to published methods (28, 29). Reversible electropermeabilization was performed at 4 kV/cm at a setting of 25-microfarad capacitance and was achieved by seven pulses using a Bio-Rad Gene Pulser Xcell electroporation system (Bio-Rad). Following electroporation, cells were incubated with antibodies for an additional 60 min at 37 °C and were centrifuged at 350 g for 20 min and resuspended in HBS prior to the experiments.

Biotinylation of Cell Surface Proteins—Aliquots of cell suspensions (1 ml) were stimulated with TG + Iono or left untreated. The reaction was terminated with ice-cold Söerscen's buffer (SB) containing 16 mM Na_2HPO_4, 114 mM NaH_2PO_4, pH 8.0. Cells were collected by centrifugation at $900 \times g$ for 13 min at 4 °C. Cell surface proteins were labeled by resuspending in EZ-Link™ Sulfo-NHS-LC-Biotin (2.5 mg/12 ml of ice-cold SB) and incubated under mixing for 1 h at 4 °C. The biotinylation reaction was terminated by the addition of 100 μl of 1 M Tris base, and remaining biotinylating agent was removed by washing the cells in ice-cold SB. Labeled cells were resuspended in PBS and then lysed in radioimmune precipitation buffer. Labeled proteins were collected by rotating the lysate overnight with streptavidin-coated agarose beads. The beads were collected by centrifugation, resuspended in Laemmli's buffer (22), boiled for 5 min, and subjected to Western blotting as described previously.

Statistical Analysis—Analysis of statistical significance was performed using Student's *t* test. $p < 0.05$ was considered to be significant for a difference.

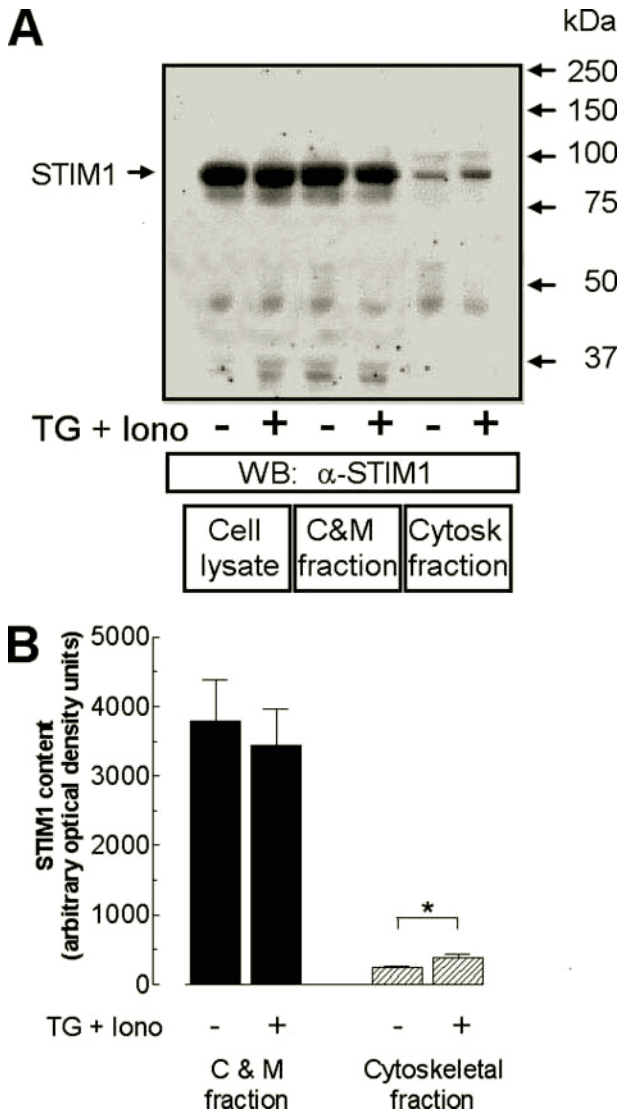

FIGURE 1. **Expression and distribution of STIM1 in human platelets.** *A*, human platelets (2×10^9 cell/ml) were incubated for 3 min in a Ca^{2+}-free medium (100 μM EGTA added) in the absence or presence of TG (1 μM) combined with Iono (50 nM) and lysed with either radioimmune precipitation buffer for whole cell lysate (*Cell lysate*) or Triton buffer to separate cytosolic and membrane fraction (*C&M fraction*) and cytoskeletal fraction (*Cytosk. fraction*). Samples were subjected to 10% SDS-PAGE and subsequent Western blotting with a specific anti-STIM1 antibody. The image shows results from one experiment representative of five others. Molecular masses indicated on the *right* were determined using molecular mass markers run in the same gel. *B*, *histograms* represent the quantification of STIM1 in the cytosolic and membrane or cytoskeletal fractions in resting (control) and TG + Iono-treated cells. Results are presented as arbitrary optical density units and expressed as mean ± S.E. *, $p < 0.05$ *versus* control.

RESULTS

Presence and Localization of STIM1 in Human Platelets—Since STIM1 has been presented as a candidate to communicate the filling state of the intracellular Ca^{2+} stores to the PM (19–21), we have tested for the presence of STIM1 in human platelet lysates by SDS-PAGE and Western blotting using an anti-STIM1 antibody, specific for the N-terminal amino acid residues 25–139 of STIM1, including the EF-hand domain (30), that has been shown to be effective in immunofluorescence studies (19). Immunoblotting of platelet whole-cell lysates with the anti-STIM1 antibody revealed the presence of STIM1 in these cells (Fig. 1*A*, *lane 1*; $n = 6$). Detection of STIM1 was not modified when cells were treated with TG (1 μM) plus Iono (50 nM) to deplete the intracellular Ca^{2+} stores (Fig. 1*A*, lane 2; $n = 6$).

We have found that STIM1 is mostly located in the cytosolic and membrane fraction and that only a small amount (about 6%) is associated with the cytoskeletal fraction (Fig. 1, *A* and *B*). To further investigate whether Ca^{2+} store depletion by TG + Iono induces association of STIM1 with the cytoskeleton,

Western immunoblot analysis was performed on the "cytoskeletal" and "cytosolic and membrane" fractions of resting and TG + Iono-stimulated platelets. Western blot analysis revealed that treatment of platelets with 1 μM TG, 50 nM Iono for 3 min significantly increases the cytoskeletal association of STIM1 (196 ± 31% of control, Fig. 1*B*; $p < 0.05$; $n = 6$) and reduced the expression of STIM1 in cytosolic and membrane fraction.

Surface Expression of STIM1—Recent studies have reported that STIM1 might be located in the membrane of the Ca^{2+} stores and at the PM (17, 20, 21). The former migrates from the intracellular Ca^{2+} stores to the PM upon depletion of the Ca^{2+} stores, where the N terminus has been suggested to face the extracellular medium, as detected by immunofluorescence and immunoelectron microscopy (19–21), suggesting that STIM1 might act as a Ca^{2+} sensor that communicates the filling state of the intracellular Ca^{2+} stores to the PM (20, 30). On the basis of the N-terminal location of the epitope recognized by the anti-STIM1 antibody, we have performed a series of immunofluorescence experiments to confirm this hypothesis and further investigate the role of $[Ca^{2+}]_i$ in this process. As shown in Fig. 2*A*, incubation of fixed, nonpermeabilized resting platelets in suspension with 1 μg/ml anti-STIM1 antibody followed by detection using an FITC-conjugated secondary antibody revealed the presence of STIM1 proteins in the cellular surface. The fluorescence observed was not due to nonspecific binding of the secondary antibody as demonstrated by the lower fluorescence detected in samples incubated with this antibody alone (<20% of the fluorescence in the presence of anti-STIM1 antibody). Data presented in Fig. 2*A* were corrected by subtraction of the fluorescence in the absence of the anti-STIM1 antibody. These findings confirm the presence of STIM1 in the PM in nonstimulated cells. To investigate whether store depletion increased surface expression of STIM1 in the PM, we repeated the experimental protocol using TG + Iono-treated cells. Treatment of human platelets with 1 μM TG, 50 nM Iono for 3 min in a Ca^{2+}-free medium (100 μM EGTA was added) significantly increased the detection of STIM1 in the PM (204 ± 38% of control; Fig. 2*A*, $p < 0.05$; $n = 6$). These findings were confirmed by biotinylation of plasma membrane proteins and collection with streptavidin-coated agarose beads. SDS-PAGE and Western blotting were used to identify STIM1. Plasma membrane expression was quantified by scanning densitometry. As shown in Fig. 2*B*, analysis of biotinylated proteins shows that STIM1 is present in the PM, and its expression significantly increases in cells stimulated with TG + Iono by 71 ± 4% ($p < 0.05$; $n = 6$).

Similar results were obtained when the studies were performed in BAPTA-loaded cells to prevent changes in $[Ca^{2+}]_i$ due to store discharge (store depletion increased the detection of STIM1 in the PM to 194 ± 37% of resting cells; Fig. 2, $p < 0.05$; $n = 6$). These findings indicate that Ca^{2+} store depletion increases surface expression of STIM1, which is independent of rises in $[Ca^{2+}]_i$. To investigate whether migration of STIM1 to the PM is supported by the actin cytoskeleton, we performed a series of experiments in the presence of Cyt D. We have previously demonstrated (24) that Cyt D is without significant effect

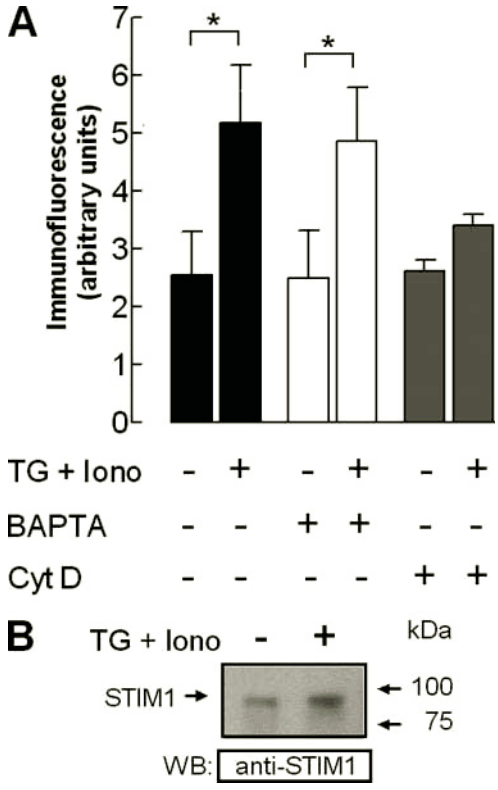

FIGURE 2. **Surface location of STIM1.** *A*, normal platelets (*black histograms*), dimethyl-BAPTA-loaded platelets (*white histograms*), or platelets incubated with cytochalasin D (10 μM; *gray histograms*) for 40 min were stimulated in a Ca^{2+}-free medium (100 μM EGTA added) for 3 min with 1 μM TG, 50 nM Iono, as indicated, and fixed with ice-cold 3% (w/v) formaldehyde in PBS for 10 min. Cells were then incubated with 1 μg/ml anti-STIM1 antibody for 2 h followed by incubation with FITC-conjugated anti-mouse IgG for a further 1 h. *Histograms* indicate the immunofluorescence values under different experimental conditions. Values are mean ± S.E. of six independent experiments. *, $p < 0.05$ *versus* control. *B*, human platelets were stimulated in a Ca^{2+}-free medium (100 μM EGTA added) with 1 μM TG, 50 nM Iono or left untreated, as indicated. Stimulation was terminated after 3 min in ice-cold Söercen's buffer, and cell surface were proteins labeled by biotinylation, as described under "Experimental Procedures." Labeled proteins were extracted with streptavidin-coated agarose beads and analyzed by SDS-PAGE and Western blotting (*WB*) using the anti-STIM1 antibody. Positions of molecular mass markers are shown on the *right*. These results are representative of four separate experiments.

on the actin filament content of nonstimulated platelets when treated for up to 40 min but effectively prevents agonist-stimulated actin filament formation. Inhibition of actin polymerization by treatment for 40 min with 10 μM Cyt D inhibited translocation of STIM1 to the PM upon Ca^{2+} store depletion by 70% (Fig. 2, $p < 0.05$; $n = 6$), suggesting that this process requires actin filament polymerization.

Association between STIM1 and hTRPC1—Platelets have been shown to endogenously express hTRPC1 channel in the PM, as well as vascular smooth muscle cells (32), and a functional interaction between IP_3RII in the Ca^{2+} stores and hTRPC1 has been presented as the most likely mechanism to account for the activation of SOCE in these cells (12, 33–35). Since STIM1 have been proposed to communicate the Ca^{2+} stores with Ca^{2+} channels in the PM, the characteristics reported make platelets an ideal cellular model to investigate the interaction between proteins in the Ca^{2+} stores and PM; therefore, we have tested for the association between STIM1

and hTRPC1 by looking for co-immunoprecipitation from platelet lysates. Immunoprecipitation and subsequent SDS-PAGE and Western blotting were conducted using control platelets and platelets in which the intracellular Ca^{2+} stores had been depleted by 3-min pretreatment with TG (1 μM) and Iono (50 nM) in the absence of extracellular Ca^{2+} (100 μM EGTA). Platelets heavily loaded with the Ca^{2+} chelator indicator dimethyl-BAPTA were used for this study so as to eliminate Ca^{2+}-dependent but not store depletion-dependent responses (12). After immunoprecipitation with anti-hTRPC1 antibody, Western blotting revealed the presence of STIM1 in samples from resting platelets. The specificity of the hTRPC1 antibody was tested with the anti-TRPC1 antibody T1E3, which has been shown to be a specific tool in the investigation of mammalian TRPC1 proteins (32, 33). We found that store depletion increased the association between STIM1 and hTRPC1 by 50% (Fig. 3*A*, *top*, *lanes 1* and *2*; $n = 6$). Similar results were observed in cells not loaded with dimethyl-BAPTA but to which a Ca^{2+}-free medium (100 μM EGTA was added at the time of the experiment; Fig. 3*A*, *top*, *lanes 3* and *4*; $n = 6$). Although no store depletion was detected by the simple addition of EGTA to platelet suspensions (data not shown), we repeated these experiments in a medium containing 200 μM $CaCl_2$ to avoid the effect of possible incipient store depletion after the addition of EGTA. As shown in Fig. 3*A*, *lanes 5* and *6*, association of STIM1 and hTRPC1 occurred in control platelets and was increased by 50% upon store depletion by TG + Iono. Western blotting of the same membranes with anti-hTRPC1 antibody confirmed a similar content of this protein in all lanes (Fig. 3*A*, *bottom*).

We also conducted converse experiments, immunoprecipitating platelet lysates with anti-STIM1 antibody and detecting for the presence of hTRPC1. After immunoprecipitation with anti-STIM1, hTRPC1 was detected in samples from control and store-depleted cells; the latter was found to be about 50% greater than control (Fig. 3*B*, *top*; $n = 6$). Immunoblot analysis of STIM1 immunoprecipitates with the same antibody as appropriate revealed a similar content of this protein in the relevant lanes (Fig. 3*B*, *bottom*). Our observations, showing an enhanced association between hTRPC1 and STIM1 in response to depletion of the intracellular Ca^{2+} stores, suggest STIM1 as a candidate for the mediation of SOCE.

Role of the Actin Cytoskeleton in the Association between STIM1 and hTRPC1—The *de novo* conformational coupling described in platelets to account for the activation of SOCE is based on the reversible interaction between elements in the ER and the PM that requires cytoskeletal reorganization (7, 12, 33, 34, 36). We have reported above that STIM1 both associates with the actin cytoskeleton and migrates to the cell surface upon store depletion, the later requiring actin remodeling. Therefore, we have explored whether the association between STIM1 and hTRPC1 is affected by inhibitors of actin polymerization, such as Cyt D. As shown in Fig. 4, treatment of dimethyl-BAPTA-loaded cells with Cyt D (10 μM) for 40 min abolished the interaction between STIM1 and hTRPC1 as detected by co-immunoprecipitation with the anti-hTRPC1 antibody and Western blotting with the anti-STIM1 antibody (*top*; $n = 4$).

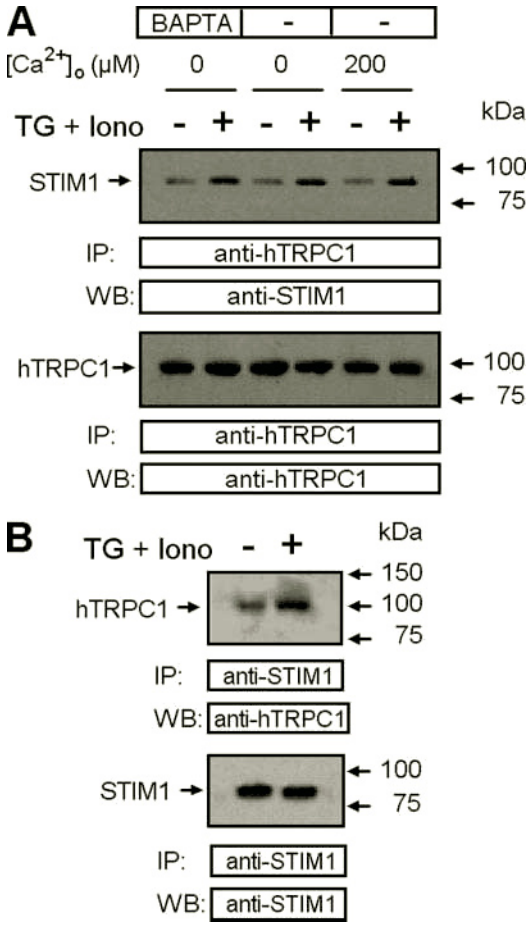

FIGURE 3. **STIM1 coimmunoprecipitates with hTRPC1 independently of changes in $[Ca^{2+}]_i$.** *A*, dimethyl-BAPTA-loaded or normal human platelets were treated, in a Ca^{2+}-free medium (100 μM EGTA added) or in a medium containing 200 μM $CaCl_2$, as indicated, with no addition (control) or with 1 μM TG and 50 nM Iono and then lysed. Whole cell lysates were immunoprecipitated (*IP*) with anti-hTRPC1 antibody. Immunoprecipitates were analyzed by Western blotting (*WB*) using anti-STIM1 antibody (*top*) and reprobed with anti-hTRPC1 antibody (*bottom*) as described under "Experimental Procedures." *B*, human platelets were treated in a Ca^{2+}-free medium (100 μM EGTA added) with no addition (control) or with 1 μM TG and 50 nM Iono and then lysed. Whole cell lysates were immunoprecipitated with anti-STIM1 antibody. Immunoprecipitates were analyzed by Western blotting using anti-hTRPC1 antibody (*top*) and reprobed with anti-STIM1 antibody as indicated. Positions of molecular mass markers are shown on the *right*. These results are representative of 4–6 independent experiments.

Western blotting of the same membranes with anti-hTRPC1 antibody confirmed a similar protein loading in all lanes (Fig. 4, *bottom*).

Inhibition of Store Depletion-evoked Interaction between STIM1 and hTRPC1 and SOCE by Electrotransjection with Anti-STIM1 Antibody—The amino acid sequence 25–139, recognized by the anti-STIM1 antibody, includes the Ca^{2+}-binding EF-hand region (30). Hence, we have investigated whether the anti-STIM1 antibody, which is directed to this sequence, could block the function of the protein. To assess this possibility, the anti-STIM1 antibody was introduced into platelets using an electropermeabilization technique. Several studies have reported that electroporation can be used successfully for transferring antibodies into cells while maintaining the physiological integrity of the cells (28, 37, 38). Human platelets were reversibly electroporated as described under "Experimental

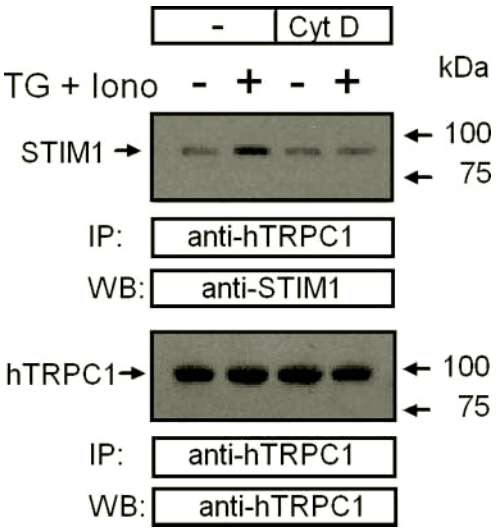

FIGURE 4. **Interaction between STIM1 and hTRPC1 requires actin filament polymerization.** Dimethyl-BAPTA-loaded human platelets were preincubated with Cyt D (10 μM) for 40 min at 37 °C and then treated in a Ca^{2+}-free medium (100 μM EGTA added) with no addition (control) or with 1 μM TG + 50 nM Iono and lysed. Whole cell lysates were immunoprecipitated (*IP*) with anti-hTRPC1 antibody. Immunoprecipitates were analyzed by Western blotting (*WB*) using anti-STIM1 antibody (*top*) and reprobed with anti-hTRPC1 antibody (*bottom*) as described under "Experimental Procedures." Positions of molecular mass markers are shown on the *right*. These results are representative of four independent experiments.

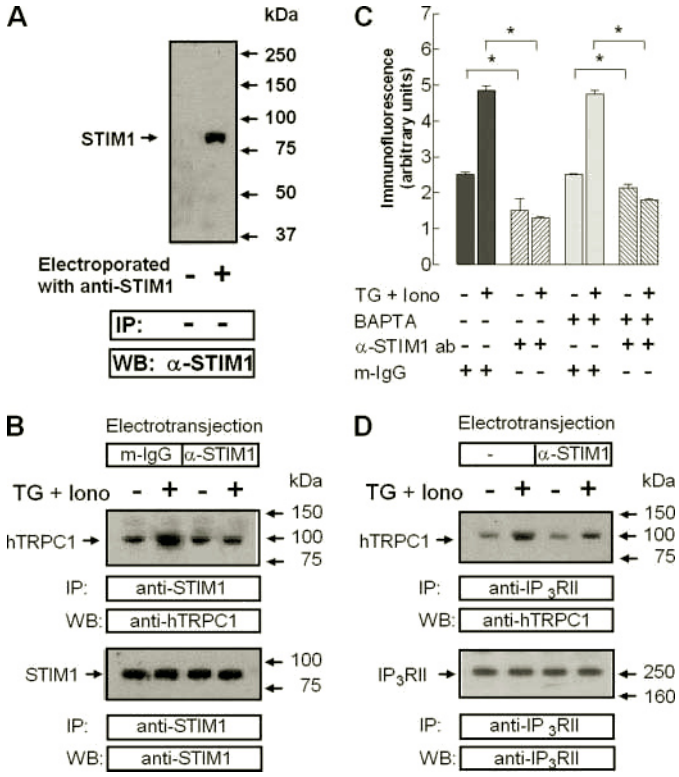

FIGURE 5. **Inhibition of store depletion-evoked interaction between STIM1 and hTRPC1, surface expression of STIM1 and coupling between hTRPC1 and IP_3RII by electrotransjection with anti-STIM1 antibody.** *A*, resting platelets (*lane 1*) or platelets electropermeabilized in a Gene Pulser as described under "Experimental Procedures" (*lane 2*) were incubated in the presence of 1 μg/ml anti-STIM1 antibody (*α-STIM1*) for 60 min as indicated and then lysed. Whole cell lysates were immunoprecipitated in the absence of antibodies but adding protein A-agarose, and immunoprecipitated proteins were analyzed by Western blotting using anti-STIM1 antibody. These results are representative of three independent experiments. *B*, human platelets (10^9 cells/ml) were electropermeabilized and incubated with 1 μg/ml mouse IgG (*m-IgG*) or with 1 μg/ml anti-STIM1 antibody (*α-STIM1*) for an additional 60 min at 37 °C, as indicated. Cells were then incubated for 3 min in the absence or presence of 1 μM TG, 50 nM Iono in a Ca^{2+}-free medium (100 μM EGTA was added) and lysed. Whole cell lysates were immunoprecipitated (*IP*) with anti-STIM1 antibody. Immunoprecipitates were analyzed by Western blotting (*WB*) using anti-hTRPC1 antibody (*top*) and reprobed with anti-STIM1 antibody (*bottom*) as described under "Experimental Procedures." Positions of molecular mass markers are shown on the *right*. These results are representative of six independent experiments. *C*, human platelets were electropermeabilized and incubated with 1 μg/ml mouse IgG (*m-IgG*) or with 1 μg/ml anti-STIM1 antibody (*α-STIM1*) for an additional 60 min at 37 °C, as indicated. Cells were stimulated in a Ca^{2+}-free medium (100 μM EGTA added) for 3 min with 1 μM TG, 50 nM Iono, as indicated, and fixed with ice-cold 3% (w/v) formaldehyde in PBS for 10 min. Cells were then incubated with 1 μg/ml anti-STIM1 antibody for 2 h followed by incubation with FITC-conjugated anti-mouse IgG for a further 1 h. *Histograms* indicate the immunofluorescence values under different experimental conditions. Values are mean ± S.E. of six independent experiments. *, $p < 0.05$ *versus* cells electroporated with mouse IgG. *D*, platelets (10^9 cells/ml) were electropermeabilized and incubated with 1 μg/ml anti-STIM1 antibody (*α-STIM1*) for an additional 60 min at 37 °C, as indicated. Cells were then incubated for 3 min in the absence or presence of 1 μM TG, 50 nM Iono in a Ca^{2+}-free medium (100 μM EGTA was added) and lysed. Whole cell lysates were immunoprecipitated with anti-IP_3RII antibody. Immunoprecipitates were analyzed by Western blotting using anti-hTRPC1 antibody (*top*) and reprobed with anti-IP_3RII antibody (*lower panel*) as described under "Experimental Procedures." Positions of molecular mass markers are shown on the *right*. These results are representative of six independent experiments.

Procedures." The presence of this antibody inside platelets was investigated in samples from control (nonelectropermeabilized) or electropermeabilized cells, both incubated with 1 μg/ml anti-STIM1 antibody, by immunoprecipitation without adding any additional anti-STIM1 antibody and subsequent Western blotting with the anti-STIM1 antibody. As shown in Fig. 5*A*, STIM1 was clearly detected in cells that had been previously electropermeabilized. Electropermeabilization allowed the anti-STIM1 antibody to enter the cells and immunoprecipitate the STIM1 protein that was then detected by Western blotting, which confirms the efficacy of the electrotransjection.

As shown in Fig. 5*B*, interaction between STIM1 and hTRPC1 was abolished in cells transjected with 1 μg/ml anti-STIM1 antibody (*top*, *lanes 3* and *4*; $n = 6$) as detected by immunoprecipitation of cell lysates with the anti-STIM1 antibody followed by Western blotting with anti-hTRPC1 antibody. To investigate the specificity of this assay, the effect of incubation with an antibody directed to a protein not related to STIM1 proteins or any other platelet protein was tested. We used a mouse IgG, since this is the nature of the anti-STIM1 antibody. Electrotransjection with 1 μg/ml mouse IgG following the protocol used for the anti-STIM1 antibody was unable to inhibit store depletion-induced interaction between STIM1 and hTRPC1 (Fig. 5*B*, *top*, *lanes 1* and *2*; $n = 6$). Reprobing of the same membranes with anti-STIM1 antibody confirmed a similar protein loading in all lanes (Fig. 5*B*, *lower panel*). Consistent with this, our results indicate that electrotransjection of anti-STIM1 antibody reduced both basal and TG + Iono-stimulated surface expression of STIM1, both in control and BAPTA-loaded cells (Fig. 5*C*; $p < 0.05$). In contrast, electrotransjection with the anti-mouse IgG antibody has a negligible effect on the surface expression of STIM1 either at resting or stimulated conditions (see Fig. 5*C versus* Fig. 2). These findings suggest that the amino acid sequence recognized by the anti-STIM1 antibody might be essential for protein function, which

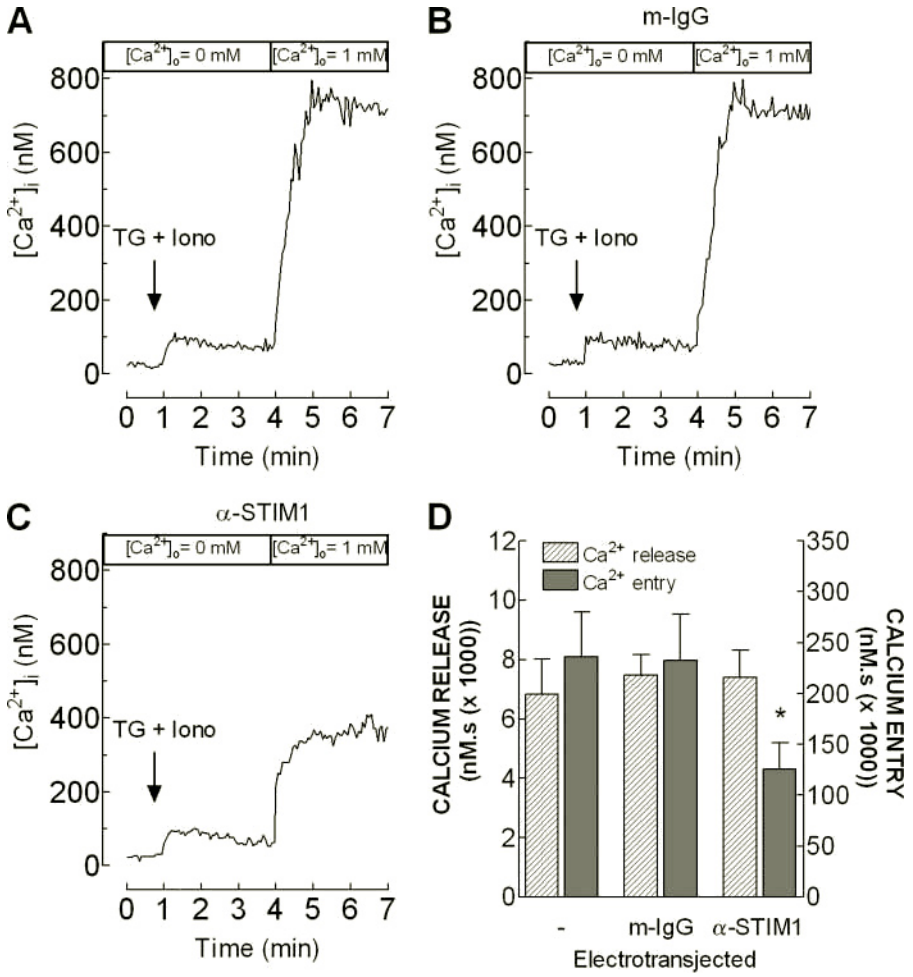

FIGURE 6. **Inhibition of store depletion-evoked SOCE by electrotransjection with anti-STIM1 antibody.** Human platelets (10^9 cells/ml) were electropermeabilized in a Gene Pulser as described under "Experimental Procedures" (*B* and *C*) or left untreated (*A*). Following electroporation, cells were incubated with 1 μg/ml mouse IgG (*B*) or with 1 μg/ml anti-STIM1 antibody (*C*) for an additional 60 min at 37 °C, loaded with fura-2, centrifuged at 350 $\times$ *g* for 20 min, and resuspended in HBS containing 200 μM $CaCl_2$. At the time of the experiment, 250 μM EGTA was added. Fura-2-loaded human platelets were stimulated with TG (1 μM) + Iono (50 nM), and 3 min later, $CaCl_2$ (final concentration 1 mM) was added to the medium ($[Ca^{2+}]_o$). Changes in fura-2 fluorescence were monitored using the 340-nm/380-nm ratio and calibrated in terms of $[Ca^{2+}]_i$. Traces are representative of 4–7 independent experiments. *D, histograms* indicate the quantification of Ca^{2+} release or entry induced by TG + Iono in control cells or cells electrotransjected with either mouse IgG (*m-IgG*) or anti-STIM1 (*α-STIM1*) antibodies. Ca^{2+} release and entry were determined as described under "Experimental Procedures." Values are means ± S.E. *, $p < 0.05$ compared with Ca^{2+} entry by TG + Iono in cells electrotransjected with mouse IgG.

depletion of the stores. At the time of the experiment 250 μM EGTA was added to perform the studies in a Ca^{2+}-free medium. In nonelectropermeabilized cells (Fig. 6*A*), TG + Iono evoked a prolonged elevation of $[Ca^{2+}]_i$, due to leakage of Ca^{2+} from intracellular stores (the integral for 3 min of the rise in $[Ca^{2+}]_i$ after the addition of TG + Iono was 6841 ± 1166 nM·s; Fig. 6*D*). The subsequent addition of Ca^{2+} (1 mM) to the external medium induced a sustained increase in $[Ca^{2+}]_i$, indicative of SOCE (the integral of the rise in $[Ca^{2+}]_i$ after the addition of $CaCl_2$ was 23,6462 ± 43,941 nM·s; Fig. 6*D*). Similar results were observed when a mouse IgG was electrotransjected into cells, suggesting that reversible electroporation *per se* or transjection of a nonspecific antibody did not alter Ca^{2+} accumulation in the stores, Ca^{2+} release, or influx in these cells. TG + Iono-induced Ca^{2+} release determined as the integral for 3 min of the rise in $[Ca^{2+}]_i$ after the addition of the agents was 7484 ± 684 nM·s, and Ca^{2+} entry measured as the integral of the rise in $[Ca^{2+}]_i$ after the addition of $CaCl_2$ was 232,354 ± 45,661 nM·s; Fig. 6, *B* and *D*). These findings also confirm the reversibility of the electroporation procedure used. Interestingly, when the anti-STIM1 antibody was electrotransjected into platelets, SOCE was significantly reduced by 46% compared with mouse IgG electrotransjected cells (the integral of the rise in $[Ca^{2+}]_i$ after the addition of $CaCl_2$ was 125,298 ± 26,116 nM·s; Fig. 6, *C* and *D*; $p < 0.05$; $n = 7$). Electrotransjection of anti-STIM1 antibody inhibited SOCE and the coupling between hTRPC1 and IP_3RII to a similar extent, which supports previous studies reporting that the coupling between hTRPC1 and IP_3RII might underlie the activation of SOCE in human platelets (33). Electrotransjection of anti-STIM1 antibody did not significantly alter TG + Iono-induced Ca^{2+} release (the integral for 3 min of the rise in $[Ca^{2+}]_i$ after the addition of TG + Iono was 7391 ± 918 nM·s; Fig. 6*D*), which indicates that electrotransjection with anti-STIM1 antibody did not impair Ca^{2+} accumulation into the intracellular stores or the ability of TG + Iono to induce store depletion (Fig. 6*C*; $p > 0.05$; $n = 7$).

must be required for migration of this protein to the PM and interaction with hTRPC1.

Furthermore, we have explored whether electrotransjection of anti-STIM1 antibody is able to alter coupling between hTRPC1 and type II IP_3R. As shown in Fig. 5*D*, in cells transjected with 1 μg/ml anti-STIM1 antibody, TG + Iono-induced interaction between hTRPC1 and IP_3RII was significantly reduced by 48%, as detected by immunoprecipitation of cell lysates with the anti-IP_3RII antibody followed by Western blotting with anti-hTRPC1 antibody ($p < 0.05$; $n = 6$).

We have further investigated whether the anti-STIM1 antibody could affect SOCE. To assess this issue, the anti-STIM1 antibody was electrotransjected into the cells, followed by depletion of the intracellular Ca^{2+} stores using TG + Iono to activate SOCE. Before the measurement of $[Ca^{2+}]_i$, cells were maintained in a medium containing 200 μM $CaCl_2$, to avoid

Recent studies have reported that application of the anti-STIM1 antibody extracellularly, which binds to the N-terminal EF hand of STIM1 located in the PM, blocks I_{CRAC} in hemato-

poietic cells and SOCE in HEK293 cells (39). To assess this possibility, human platelets were incubated for 30 min with anti-STIM1 antibody (1 μg/ml) followed by depletion of the intracellular Ca^{2+} stores using TG + Iono to activate SOCE. As depicted in Fig. 7, *A* and *B*, incubation of platelets with anti-STIM1 antibody for 30 min decreased Ca^{2+} entry by 36 ± 10% (the integral of the rise in $[Ca^{2+}]_i$ after the addition of $CaCl_2$ was 231,421 ± 10,516 and 148,109 ± 25,514 nM·s in control and anti-STIM1 antibody-treated cells, respectively; $p < 0.05$). Incubation for 30 min with anti-STIM1 antibody did not significantly alter TG + Iono-induced Ca^{2+} release from the intracellular stores (the integral for 3 min of the rise in $[Ca^{2+}]_i$ after the addition of TG + Iono was 7863 ± 1110 and 6938 ± 158 nM·s in control and anti-STIM1 antibody-treated cells, respectively). In contrast, application of the anti-STIM1 antibody extracellularly was unable to impair surface expression of STIM1 either at resting conditions or upon stimulation with TG + Iono (Fig. 7*C*; $p > 0.05$; $n = 4$).

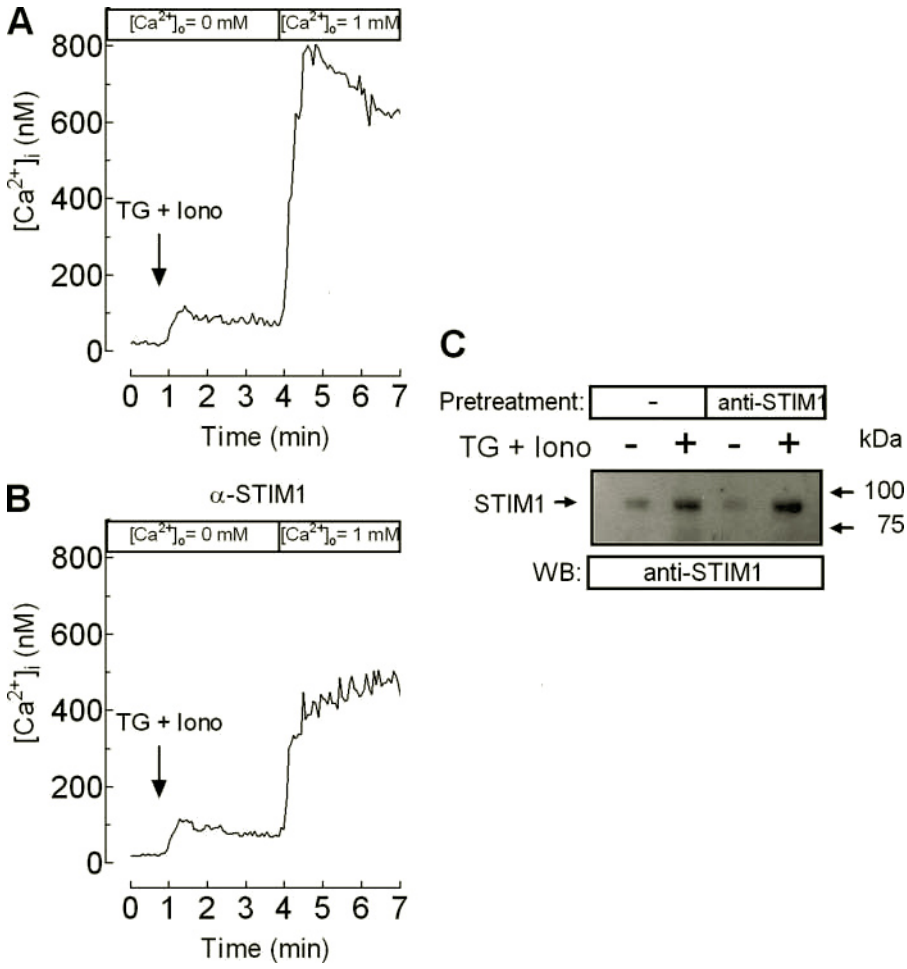

FIGURE 7. **Effect of extracellular anti-STIM1 antibody on store depletion-evoked SOCE and surface expression of STIM1.** *A* and *B*, human platelets (10^9 cells/ml) were incubated with 1 μg/ml anti-STIM1 antibody for 30 min at 37 °C (*B*) or left untreated (*A*). At the time of the experiment, 250 μM EGTA was added. Fura-2-loaded human platelets were stimulated with TG (1 μM) + Iono (50 nM), and 3 min later, $CaCl_2$ (final concentration 1 mM), was added to the medium. Changes in fura-2 fluorescence were monitored using the 340-nm/380-nm ratio and calibrated in terms of $[Ca^{2+}]_i$. Traces are representative of five independent experiments. *C*, human platelets were incubated with 1 μg/ml anti-STIM1 antibody for 30 min at 37 °C or left untreated as indicated. Cells were then stimulated in a Ca^{2+}-free medium (100 μM EGTA added) in the absence or presence of 1 μM TG, 50 nM Iono, as indicated. Stimulation was terminated after 3 min in ice-cold Söercen's buffer, and cell surface proteins were labeled by biotinylation, as described under "Experimental Procedures." Labeled proteins were extracted with streptavidin-coated agarose beads and analyzed by SDS-PAGE and Western blotting using the anti-STIM1 antibody. Positions of molecular mass markers are shown on the *right*. These results are representative of four separate experiments.

DISCUSSION

Most cell types modulate a number of cellular functions by the generation of Ca^{2+} signals, which consist of spatio-temporal modifications of $[Ca^{2+}]_i$. These signals involve Ca^{2+} release from intracellular stores and Ca^{2+} entry through PM channels. Among the Ca^{2+} entry pathways described, SOCE, regulated by the Ca^{2+} content in the stores (11), is one of the most ubiquitous and a major mechanism for Ca^{2+} influx in excitable and nonexcitable cells. Whereas the messengers involved in the release of Ca^{2+} from intracellular compartments and the channels present in the membrane of the stores have long been identified, the precise mechanism involved in the communication between the Ca^{2+} stores and PM channels has not been fully elucidated. Recent studies using RNAi-based techniques and mutant proteins have presented STIM1 as a candidate messenger linking the Ca^{2+} content in the stores with the activation of SOCE (18, 19, 21). STIM1 has been reported to modulate I_{CRAC} by interaction with the Ca^{2+} release-activated Ca^{2+} modulators Orai1 or Orai2 (40, 41). Here, we present for the first time evidence for the interaction of STIM1 with endogenously expressed human canonical TRP1 (hTRPC1) in platelets, where this channel has been shown to conduct Ca^{2+} entry during SOCE. This interaction was found to be independent of rises in cytosolic free Ca^{2+} concentration but dependent on store depletion, which parallels the characteristics of SOCE. Supporting these findings, immunofluorescence and biotinylation assays have reported that STIM1 translocates to the PM upon store depletion, which might lead to the enhanced interaction with hTRPC1 under these conditions. Functional knock-down of STIM1 by electrotransjection of cells with anti-STIM1 antibody, directed toward the N-terminal sequence that includes the Ca^{2+}-binding region, prevented the migration of STIM1 toward the PM, the interaction between STIM1 and hTRPC1, coupling between hTRPC1 and IP_3RII, and subsequently reduced SOCE, which provides further evidence for the functional significance of the interaction between STIM1 and hTRPC1.

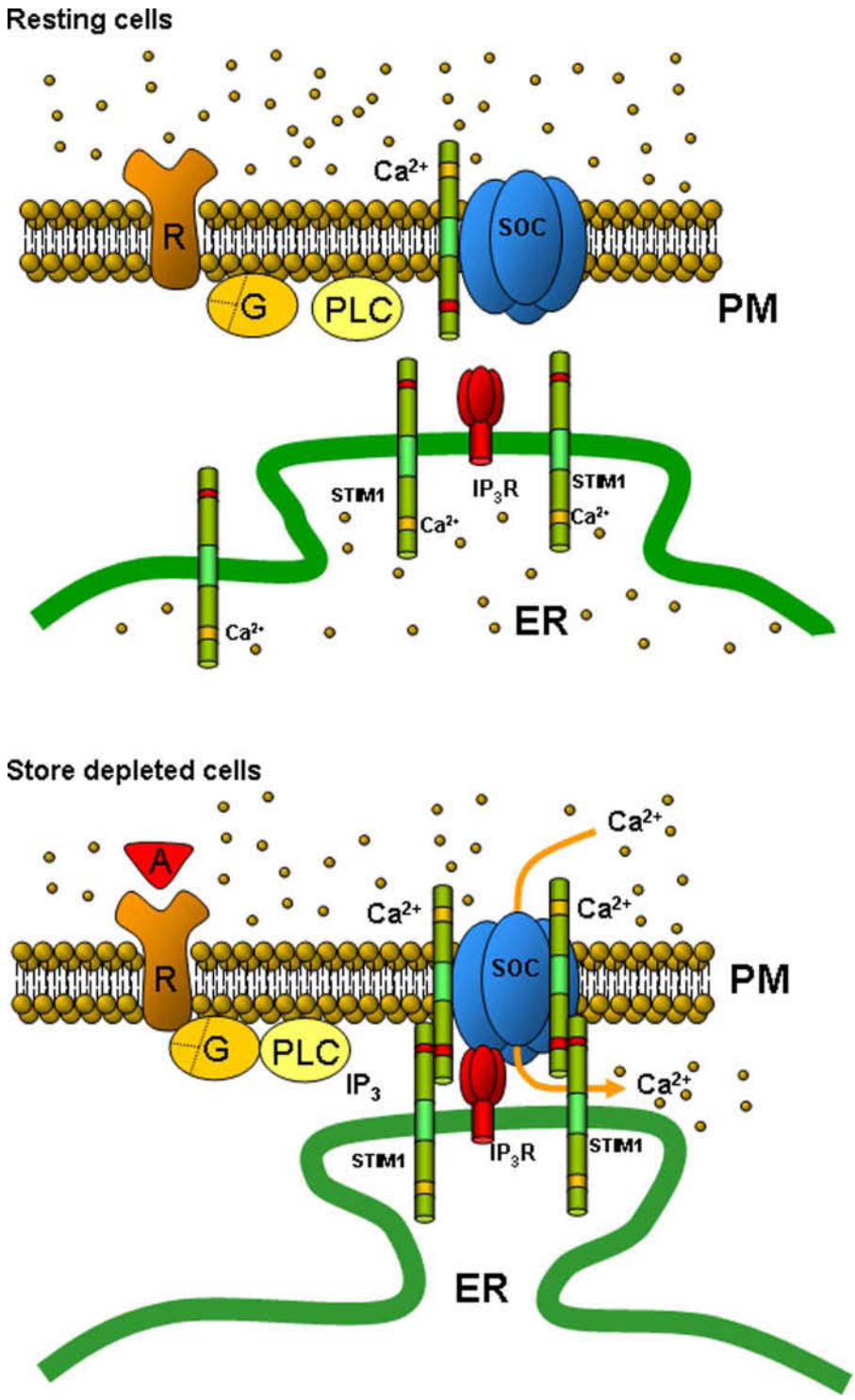

FIGURE 8. **Speculative model for the role of STIM1 in the activation of SOCE in platelets.** *Top*, in cells with replete Ca^{2+} stores, STIM1 is localized throughout the ER membrane (20, 21, 31) and also in the PM, and store-operated channels (*SOC*) are inactive. *Bottom*, cell activation begins with the occupation of a membrane receptor (*R*) by an agonist (*A*), leading to activation of phospholipase C (*pLC*), through a G-protein (*G*). PLC activation results in the synthesis of inositol 1,4,5-trisphosphate (IP_3), which activates the IP_3R and induces Ca^{2+} release from the ER. The decrease in stored Ca^{2+} might be communicated to the PM SOC by a mechanism that involves STIM1 in the ER, PM, or both. STIM1 contains an EF-hand region (shown in *yellow*) facing the lumen of the ER and the extracellular medium, which might be essential for sensing ER or extracellular Ca^{2+} concentrations. After store depletion, STIM1 located in the ER unbinds Ca^{2+} and either translocates to the PM or remains in the ER membrane, where it promotes the interaction between the ER and the PM to facilitate *de novo* coupling between the IP_3RII and the SOC hTRPC1 already located in the PM, which might result in the activation of SOCE.

In addition, we have found that external application of anti-STIM1 antibody reduces TG + Iono-evoked SOCE. These data, together with the effect of internal application of the anti-STIM1 antibody, reveal that STIM1 might play an important role in the regulation of SOCE. Since the inhibition of Ca^{2+} influx by internal or external application of anti-STIM1 antibody is similar, the inhibition of SOCE might be mediated by binding of the antibody to PM-associated STIM1. In fact, STIM1 at the PM has been shown to exert a control on the operation of Ca^{2+} channels (39). However, this interpretation does not entirely explain some of the effects observed after electrotransjection with the antibody, such as the impairment of the translocation of STIM1 to the PM observed in cells electrotransjected with the anti-STIM1 antibody, which has not been observed after external application of the antibody to nonelectropermeabilized cells. Therefore, we cannot rule out the possibility that the effects of electrotransjection of the anti-STIM1 antibody on SOCE are mediated by binding of the antibody to intracellular STIM1. The anti-STIM1 antibody used recognizes the amino acid sequence 25–139, located in the N terminus, which, when STIM1 is located in the plasma membrane or intracellular membranes, is not accessible from the cytosol. Our results suggest that at rest, the ER-associated pool of STIM1 might be cycling between the ER and the cytosol, and the PM pool must be cycling between the PM and the cytosol. This process might expose the N-terminal sequence to the anti-STIM1 antibody, which is present in the cells for 60 min before the performance of the experiments, resulting in the impairment of STIM1 cellular functions. This hypothesis is supported by a previous study by Manji *et al.* (17), reporting that STIM1 antibodies generated to the N-terminal and the C-terminal sequences were

both able to detect STIM1 in the cytoplasm of chronic myeloid leukemia cells (K562). In addition, we have found that when cells were electrotransjected with anti-STIM1 antibody, but not with a nonspecific mouse IgG, surface expression of STIM1 is reduced at resting conditions, which further supports that STIM1 located in the PM might be cycling between the PM and the cytosol, where it is accessible to the anti-STIM1 antibody. It is also expected that any mechanism that accelerates the cycling activity, such as cell stimulation with TG + Iono, enhances the exposure of STIM1 to the anti-STIM1 antibody. Consistent with this, we have found that treatment of cells electrotransjected with anti-STIM1 antibody with TG + Iono resulted in a reduction in surface expression of this protein.

We have previously shown coupling between IP_3RII and hTRPC1 only after depletion of the intracellular Ca^{2+} stores and not at resting conditions (12, 33). In cells electroporated, we have detected little co-immunoprecipitation between hTRPC1 and IP_3RII in nonstimulated cells, which seems to be a result of the electroporation itself, independent of store depletion, since basal $[Ca^{2+}]_i$ and the amount of Ca^{2+} accumulated into the intracellular stores were found to be similar in control and electroporated cells. Electrotransjection of cells with anti-STIM1 antibody significantly reduced the coupling between IP_3RII and hTRPC1, which supports the role of STIM1 in the activation of SOCE in human platelets.

Here we show interaction between STIM1 and hTRPC1 in resting platelets, which is enhanced upon store depletion. Functional STIM1 seems to be required for coupling between hTRPC1 and type II IP_3R. Although speculative, a possible explanation for these findings resides in a role for STIM1 bridging the stores and the PM. Thus, the PM pool of STIM1 under resting conditions might form stable complexes with Ca^{2+} channels and other Ca^{2+}-related proteins in functional microdomains involved in Ca^{2+} signaling. Store depletion significantly enhances the PM pool and may induce homo-oligomerization of STIM1 in the Ca^{2+} stores and STIM1 located in the PM, which, in turn, might mediate the interaction between both membranes, as previously suggested (19, 20). Both mechanisms, association of STIM1 in the PM with hTRPC1 and oligomerization of hTRPC1-associated STIM1 with STIM1 located in the Ca^{2+} stores, might explain an increase in the interaction between hTRPC1 and STIM1 detected by co-immunoprecipitation.

Our findings suggest that fully functional STIM1 is necessary for the activation of SOCE in platelets, a mechanism that is probably mediated by interaction with hTRPC1 in the PM to mediate the communication of the filling state of the Ca^{2+} stores to the Ca^{2+} channels in the PM and to exert a control over the operation of these channels (a schematic diagram of the proposed model is depicted in Fig. 8). These data are compatible with an important role for STIM1 in the activation of SOCE by *de novo* coupling of IP_3RII to hTRPC1, which we have suggested may underlie the activation of SOCE in human platelets (7, 12, 33, 34, 42). Whether STIM1 plays a role as a luminal Ca^{2+} sensor in store depletion-induced actin cytoskeleton reorganization and the subsequent trafficking of the Ca^{2+} stores to the PM deserves further studies.

Acknowledgment—We thank Mercedes Gomez Blázquez for technical assistance.

REFERENCES

1. Camello, C., Pariente, J. A., Salido, G. M., and Camello, P. J. (2000) *Curr. Biol.* **10,** 161–164
2. Berridge, M. J., Bootman, M. D., and Roderick, H. L. (2003) *Nat. Rev. Mol. Cell. Biol.* **4,** 517–529
3. Berridge, M. (2004) *Sci. STKE 2004*, pe33
4. Putney, J. W., Jr., Broad, L. M., Braun, F. J., Lievremont, J. P., and Bird, G. S. (2001) *J. Cell Sci.* **114,** 2223–2229
5. Putney, Jr. J. W. (2004) *Sci. STKE 2004*, pe37
6. Bolotina, V. M., and Csutora, P. (2005) *Trends. Biochem. Sci.* **7,** 378–387
7. Rosado, J. A., Redondo, P. C., Sage, S. O., Pariente, J. A., and Salido, G. M. (2005) *J. Cell. Physiol.* **205,** 262–269
8. Zhu, X., Jiang, M., Peyton, M., Boulay, G., Hurst, R., Stefani, E., and Birnbaumer, L. (1996) *Cell* **85,** 661–671
9. Boulay, G., Brown, D. M., Qin, N., Jiang, M., Dietrich, A., Zhu, M. X., Chen, Z., Birnbaumer, M., Mikoshiba, K., and Birnbaumer, L. (1999) *Proc. Natl. Acad. Sci. U. S. A.* **96,** 14955–14960
10. Putney, J. W., Jr., and McKay, R. R. (1999) *BioEssays* **21,** 38–46
11. Putney, J. W., Jr. (1999) *Proc. Natl. Acad. Sci. U. S. A.* **96,** 14669–14671
12. Rosado, J. A., and Sage, S. O. (2000) *Biochem. J.* **350,** 631–635
13. Yuan, J. P., Kiselyov, K., Shin, D. M., Chen, J., Shcheynikov, N., Kang, S. H., Dehoff, M. H., Schwarz, M. K., Seeburg, P. H., Muallem, S., and Worley, P. F. (2003) *Cell* **114,** 777–789
14. Treves, S., Franzini-Armstrong, C., Moccagatta, L., Arnoult, C., Grasso, C., Schrum, A., Ducreux, S., Zhu, M. X., Mikoshiba, K., Girard, T., Smida-Rezgui, S., Ronjat, M., and Zorzato, F. (2004) *J. Cell Biol.* **166,** 537–548
15. Stamboulian, S., Moutin, M. J., Treves, S., Pochon, N., Grunwald, D., Zorzato, F., De Waard, M., Ronjat, M., and Arnoult, C. (2005) *Dev. Biol.* **286,** 326–337
16. Hisatsune, C., and Mikoshiba, K. (2005) *Sci. STKE 2005*, pe53
17. Manji, S., Sparker, N. J., Williams, R. T., van Stekelenburg, L., Pearson, R. B., Dziadek, M., and Smith, P. J. (2000) *Biochim. Biophys. Acta.* **1481,** 147–155
18. Liou, J., Kim, M. L., Heo, W. D., Jones, T. J., Myers, J. W., Ferrell, J. E., Jr., and Meyer, T. (2005) *Curr. Biol.* **15,** 1235–1241
19. Roos, J., DiGregorio, P. J., Yeromin, A. V., Ohlsen, K., Lioudyno, M., Zhang, S., Safrina, O., Kozak, J. A., Wagner, S. L., Cahalan, M. D., Velicelebi, G., and Stauderman, K. A. (2005) *J. Cell Biol.* **169,** 435–445
20. Putney, J. W., Jr. (2005) *J. Cell Biol.* **169,** 381–382
21. Zhang, S. L., Yu, Y., Roos, J., Kozak, J. A., Deerinck, J. T., Ellisman, M. H., Stauderman, K. A., and Cahalan, M. D. (2005) *Nature* **437,** 902–905
22. Rosado, J. A., Jenner, S., and Sage, S. O. (2000) *J. Biol. Chem.* **275,** 7527–7533
23. Grynkiewicz, G., Poenie, M., and Tsien, R. Y. (1985) *J. Biol. Chem.* **260,** 3440–3450
24. Rosado, J. A., and Sage, S. O. (2000) *Biochem. J.* **347,** 183–192
25. Heemskerk, J. W., Feijge, M. A., Henneman, L., Rosing, J., and Hemker, H. C. (1997) *Eur. J. Biochem.* **249,** 547–555
26. Rosado, J. A., Graves, D., and Sage, S. O. (2000) *Biochem. J.* **351,** 429–437
27. Laemmli, U. K. (1970) *Nature* **227,** 680–685
28. Dhar, A., and Shukla, S. D. (1994) *J. Biol. Chem.* **269,** 9123–9127
29. Scrutton, M. C., Knight, D. E., and Authi, K. S. (1996) in *Platelets* (Watson, S. P., and Authi, K. S., eds) pp. 47–66, IRL Press, Oxford
30. Williams, R. T., Manji, S. S., Parker, N. J., Hancock, M. S., Van Stekelenburg, L., Eid, J. P., Senior, P. V., Kazenwadel, J. S., Shandala, T., Saint, R., Smith, P. J., and Dziadek, M. A. (2001) *Biochem. J.* **357,** 673–685
31. Marchant, J. S. (2005) *Curr. Biol.* **15,** R493–R495
32. Xu, S. Z., and Beech, D. J. (2001) *Circ. Res.* **88,** 84–87
33. Rosado, J. A., Brownlow, S. L., and Sage, S. O. (2002) *J. Biol. Chem.* **277,** 42157–42163
34. Brownlow, S. L., and Sage, S. O. (2003) *Biochem. J.* **375,** 697–704

35. Ben Amor, N., Redondo, P. C., Bartegi, A., Pariente, J. A., Salido, G. M., and Rosado, J. A. (2006) *J. Physiol.* **570,** 309–323
36. Redondo, P. C., Lajas, A. I., Salido, G. M., Gonzalez, A., Rosado, J. A., and Pariente, J. A. (2003) *Biochem. J.* **370,** 255–263
37. Chakrabarti, R., Wylie, D. E., and Schuster, S. M. (1989) *J. Biol. Chem.* **264,** 15494–15500
38. Wilson, A. K., Horwitz, J., and De Lanerolle, P. (1991) *Am. J. Physiol.* **260,** C355–C363
39. Spassova, M. A., Soboloff, J., He, L.-P., Xu, W., Dziadek, M. A., and Gill, D. L. (2006) *Proc. Natl. Acad. Sci. U. S. A.* **103,** 4040–4045
40. Peinelt, C., Vig, M., Koomoa, D. L., Beck, A., Nadler, M. J., Koblan-Huberson, M., Lis, A., Fleig, A., Penner, R., and Kinet, J. P. (2006) *Nat. Cell Biol.* **8,** 771–773
41. Mercer, J. C., DeHaven, W. I., Smyth, J. T., Wedel, B., Boyles, R. R., Bird, G. S., and Putney, J. W., Jr. (June 28, 2006) *J. Biol. Chem.* **281,** 24979–24990
42. Rosado, J. A., and Sage, S. O. (2001) *Biochem. J.* **356,** 191–198